A Comparative Study of Two Wavelet-Based Numerical Schemes for the Solution of Nonlinear Boundary Value Problems

Harinakshi Karkera, Sharath Kumar Shettigar and Nagaraj N Katagi

***Abstract*—The study aims to explore wavelet applications for analyzing nonlinear boundary value problems. Although several wavelet methods are reviewed in the literature, a comparative study of their strengths and limitations has found only a few attempts. This study bridges the gap between two wavelet-based numerical methods, namely, higher order Daubechies wavelet-based Galerkin method and Haar wavelet collocation method, by conducting a comparative study. Nonlinear boundary value problems arising in mathematical physics are solved using both schemes, followed by the computation of optimal error estimates. Furthermore, the advantages offered by the Haar wavelet collocation method over the wavelet-Galerkin method and the rate of convergence are also discussed in detail.**

***Index Terms*—Haar wavelets, Wavelet-Galerkin method, Boundary value problems, Error estimates.**

I. Introduction

THE advancement in modern numerical methods for differential equations pushes one to extract qualitative information about the behavior of solutions, convergence, efficiency in tackling natural nonlinearity, etc. rather than just finding a solution or quantitative information about it. This shift from the quantitative to the qualitative is reflected in a shift in the mathematical techniques used to analyze differential equations. In this regard, wavelet-based numerical approaches are a revolutionary evolution.

Wavelets are a powerful mathematical tool with numerous applications in practical fields including signal and image processing, optimization problems, data compression, etc. The ability to simultaneously optimize time and frequency resolutions is a significant advantage of utilizing wavelets for signal processing. Wavelets are also extremely useful to solve and analyze differential equations arising in numerous mathematical modeling problems. The wavelet technique permits the division of a complicated function into several simpler ones and their separate analysis.

Among the different wavelet families, Haar wavelets are mathematically the simplest, and historically the first example of real-valued wavelets with an explicit expression for its scaling and wavelet functions. In 1910, Alfred Haar used rectangular type of orthonormal basis functions instead of the sine and cosine basis functions and introduced the Haar function as a group of square waves with magnitude ± 1 in some finite intervals that vanish outside the interval. Haar wavelet methods have had great success in solving several linear and nonlinear problems of engineering interest. Chen and Hsiao [1] were the first to derive the operational matrix for Haar wavelets and demonstrated its application for solution of integral/differential equations. They accomplished this by expanding the highest derivative appearing in the problem in terms of Haar series and obtaining all other derivatives using integration. Later, Lepik [2] employed the algorithm with uniform grid. Chang [3] applied the Haar wavelet method to solve ordinary differential equations with initial or boundary conditions. Subsequently, many investigators have expanded on the work of Lepik for various model integral and differential equations [4]–[6]. Due to their simplicity, Haar wavelet-based numerical methods have attained distinctive attention among wavelet families and have become a useful tool for solving several problems of differential and integral equations.

Another well-known family of wavelets is the Daubechies wavelet functions, which are compactly supported, differentiable, and form an orthonormal basis of $L^2(\mathbb{R})$, discovered by Ingrid Daubechies [7]. It is interesting to note that these functions combine orthogonality with localization (i.e. compact support) and scaling properties, which are beneficial for the numerical solution of differential equations. Also, this family of Daubechies wavelets includes members from highly localized to highly smooth. More significantly, finite linear combinations of Daubechies wavelets offer local pointwise representations of low-degree polynomials, which is one of the interesting features of this wavelet.

The pioneering work on exploring the wavelet-Galerkin method was initiated by Glowinski *et al.* [8]. They considered the dilates of translated Daubechies scaling functions with support $(0, L-1)$ and restricted it to $(0, 1)$. Latto *et al.* [9] proposed methods for evaluation of connection coefficients (both single term and multiple term) on unbounded intervals. Romine and Peyton [10] modified the connection coefficients obtained by Latto *et al.* [9] at the boundaries and derived the proper connection coefficients on bounded intervals. Amaratunga *et al.* [11] applied wavelet-Galerkin technique for the solution of one-dimensional partial differential equations. Lu *et al.* [12] proposed a fictitious boundary approach for treating different types of boundary conditions in the solution of differential equations. Recently, Choudhury and Deka [13] further generalized the approach given in [8] for arbitrary domain (a, b) and obtained the numerical solutions for

Manuscript received September 18, 2023; revised March 9, 2024.

Harinakshi Karkera is an assistant professor in the Department of Mathematics, Manipal Institute of Technology, Manipal Academy of Higher Education, Manipal-576104, India. (e-mail: harinakshi.karkera@manipal.edu).

Sharath Kumar Shettigar is a research scholar in the Department of Mathematics, Manipal Institute of Technology, Manipal Academy of Higher Education, Manipal-576104, India. (e-mail: sharath.shettigar@learner.manipal.edu).

Nagaraj N. Katagi is a professor in the Department of Mathematics, Manipal Institute of Technology, Manipal Academy of Higher Education, Manipal-576104, India. (Corresponding author, e-mail: nn.katagi@manipal.edu).

one-dimensional elliptic problems of order two. Priyadarshi and Kumar [14] demonstrated the wavelet-Galerkin solution for fourth-order differential equations, Da Silva *et al.* [15] studied the propagation of electromagnetic waves and later Černá and Finěk [16] solved integral and integro-differential equations using wavelet-Galerkin method. Ganga *et al.* utilized wavelet-Galerkin method to study the Blasius flow problem. Bin Jebreen and Dassios [17] implemented the method to solve fractional order Riccati equation. Very recently, Rostami [18] applied wavelet-Galerkin method to solve Volterra equations, and Koksal [19] analyzed telegraph equations using wavelet-Galerkin method.

Our primary contribution in this work is three-fold. Firstly, we brief the general solution procedure of wavelet-Galerkin method (WGM) and Haar wavelet collocation method (HWCM) for differential equations. Secondly, we exemplify the concrete implementation process of applying the two proposed methods for the solution of some nonlinear second-order boundary value problems and carry out the error analysis. We compare the two strategies using two essential criteria: effort spent on implementation and accuracy of the solution. We also explore the rate of convergence of HWCM. Lastly, we draw some potential observations of the two methods. The insights from this comparative study can be further developed to analyze the higher-order nonlinear problems.

This paper is structured as follows: A short introduction to Haar wavelets and Daubechies wavelets is given in Section II. Section III illustrates the method of solution of wavelet-Galerkin and Haar wavelet collocation approaches. Section IV discusses some case studies through the proposed methods. Important concluding remarks are reported in Section V.

II. Preliminaries

A. Haar wavelets

The Haar scaling function $h_1(t)$ is defined as

$$h_1(t) = \begin{cases} 1, & t \in [0,1) \\ 0, & \text{elsewhere.} \end{cases} \tag{1}$$

The Haar mother wavelet is derived as the linear combination of the Haar scaling function:

$$h_2(t) = h_1(2t) - h_1(2t-1). \tag{2}$$

The family of Haar wavelets is constructed from the single function $h_2(t)$ by applying translations and scalings:

$$h_{i_H}(t) \quad = \quad h_2(2^j t - k) = \begin{cases} 1, & t \in [a,b) \\ -1, & t \in [b,c) \\ 0, & \text{elsewhere} \end{cases} \tag{3}$$

where

$$a = \frac{k}{m}, \qquad b = \frac{k+0.5}{m}, \qquad c = \frac{k+1}{m},$$

and the dilation parameter $j = 0, 1, \ldots, J$ measures degree of compression. J is the level of resolution of the wavelet. The support of wavelet decreases as j increases. $k = 0, 1, \ldots, m-1$ stands for the translation parameter which signifies the location of the particular function, where $m = 2^j$. The wavelet number $i = m + k + 1$ takes the lowest value 2 (that is $k = 0,\ m = 1$) and the highest value 2^{J+1}. The value $i = 1$ corresponds to the Haar scaling function defined in Eqn.(1).

Observe that, each Haar wavelet function $h_i(t)$ vanishes outside the interval $I = [a, c)$. The length of the interval I is 2^{-j} and so for larger j, the length of I decreases. Therefore, based on the context, the function $h_i(t)$ is well localized in time or space. This property is to be contrasted with the trigonometric basis $\{e^{2\pi i n t}\}_{n\in\mathbb{Z}}$. Note that each element of the trigonometric basis has an absolute value of 1 for every $t \in [0, 1)$, and so it never vanishes for any t. Graphical construction of the first eight Haar wavelets and their integrals are shown in Fig.1.

B. Daubechies wavelets

The Daubechies scaling function is defined as

$$\phi(t) = \sqrt{2} \sum_{k=0}^{L-1} c_k \phi(2t-k), \tag{4}$$

where $\phi(t)$ is normalized (i.e. $\int_{-\infty}^{\infty} \phi(t)dt = 1$). L is an even positive integer called the genus (or order) of the Daubechies wavelet. The coefficients $c_k, k = 0, 1, \ldots, L-1$ are called low-pass filter coefficients. The Daubechies mother wavelet is defined in terms of the scaling function as

$$\psi(t) = \sqrt{2} \sum_{k=0}^{L-1} d_k \phi(2t-k), \tag{5}$$

where $d_k, k = 0, 1, \ldots, L-1$ are called high-pass filter coefficients. The filter coefficients c_k and d_k are connected by the relation $d_k = (-1)^k c_{L-1-k}, k = 0, 1, \ldots, L-1$, and are derived so as to satisfy the following conditions:

(i) $c_k = 0$ for $k \notin \{0, 1, 2, \ldots, L-1\}$
(ii) $\sum_{k=0}^{L-1} c_k = \sqrt{2}$
(iii) $\sum_{k=0}^{L-1} c_k c_{k-m} = \delta_{0,m}$
(iv) $\sum_{k=0}^{L-1} (-1)^k k^m c_k = 0, \quad m = 0, 1, \ldots \frac{L}{2} - 1$

where $\delta_{0,m}$ is the Kronecker delta function. The sets $\left\{\phi_{j,k}(t) = 2^{j/2}\phi(2^j t - k) | j, k \in \mathbb{Z}\right\}$ and $\left\{\psi_{j,k}(t) = 2^{j/2}\psi(2^j t - k) | j, k \in \mathbb{Z}\right\}$ obtained by dilation and translation of $\phi(t)$ and $\psi(t)$ forms orthonormal bases. The support of Daubechies scaling function $\phi(t)$ and wavelet $\psi(t)$ are $\text{supp}(\phi) = \text{supp}(\psi) = [0, L-1]$. Also, the Daubechies wavelet has $L/2$ vanishing moments. In fact, the Haar wavelet discussed in Section II-A is the simplest Daubechies wavelet with two filter coefficients (i.e. $c_0 = c_1 = 1$) and one vanishing moment (and hence denoted as $db1$). When $L = 4$, the filter coefficients for Daubechies wavelets are

$$\begin{aligned} c_0 &= \frac{1+\sqrt{3}}{4\sqrt{2}} \ ; \qquad d_0 = \frac{1-\sqrt{3}}{4\sqrt{2}} \\ c_1 &= \frac{3+\sqrt{3}}{4\sqrt{2}} \ ; \qquad d_1 = \frac{\sqrt{3}-3}{4\sqrt{2}} \\ c_2 &= \frac{3-\sqrt{3}}{4\sqrt{2}} \ ; \qquad d_2 = \frac{3+\sqrt{3}}{4\sqrt{2}} \\ c_3 &= \frac{1-\sqrt{3}}{4\sqrt{2}} \ ; \qquad d_3 = \frac{-1-\sqrt{3}}{4\sqrt{2}}. \end{aligned}$$

The graphs of $\phi(t)$ and $\psi(t)$ for $L = 4, 8, 12, 16$ are plotted in Fig.2. The Daubechies wavelets do not exhibit symmetry

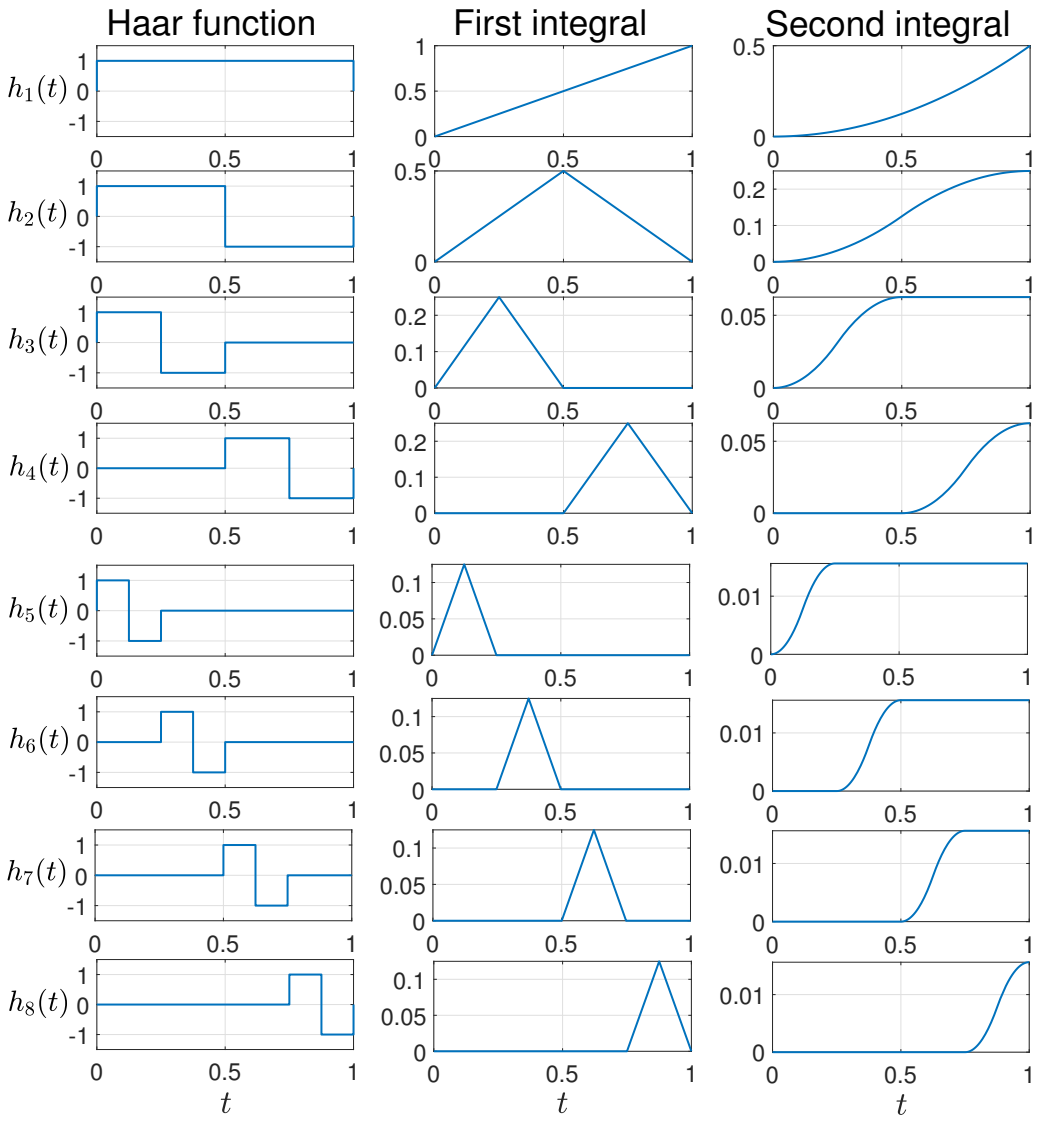

Fig. 1: First eight Haar wavelets and their integrals

or antisymmetry for $L > 2$ but, their smoothness (regularity) increases with L.

Unlike Haar wavelets, Daubechies wavelets do not have an explicit expression for the basic scaling function and wavelet. However, different approaches such as cascade algorithm, subdivision scheme, Daubechies-Lagarias algorithm, successive approximation [7], [20], etc., are well documented for direct evaluation of $\phi(t)$ and $\psi(t)$ at dyadic rational points. Due to the unavailability of explicit forms for $\phi(t)$ and $\psi(t)$, analytical integration or differentiation is not possible. This complicates the procedure for solution of differential equations which includes integral or product of nonlinear terms. Although this shortcoming is overcome through the concept of connection coefficients (discussed in the Appendix), the calculation of connection coefficients [9] is a tedious task and must be performed separately for various types of integrals.

III. Method of Solution

In this section, we implement the HWCM and WGM for the solution of nonlinear boundary value problems of the form

$$f\left(t, u(t), u'(t), u''(t)\right) = 0\,, \qquad 0 \le t \le 1\,, \tag{6}$$

with boundary conditions

$$u(0) = \alpha\,, \qquad u(1) = \beta\,, \tag{7}$$

where f is a nonlinear function. The Daubechies scaling functions are employed as basis functions for Galerkin solutions of some special cases of Eq.(6).

A. Haar wavelet collocation method (HWCM):

By definition, the Haar wavelet function is not continuous and so it is not possible to directly apply it for the solution of differential equations. But, as displayed in fig.1, the integrals of Haar wavelet are continuous. Therefore the highest derivative appearing in the problem equation is approximated usig Haar wavelet and the lower derivatives are obtained by integration. This ensures that the required unknown function is approximated using a higher Haar integral, which is known to be smooth. Following the approach introduced by Chen and Hsiao [1], the integrals of Haar wavelet are given as

$$\begin{aligned} p_{1,i}(t) &= \int_0^t h_i(t)dt \\ p_{v,i}(t) &= \int_0^t p_{v-1,i}(t)dt, \quad v = 2, 3, \dots \end{aligned} \tag{8}$$

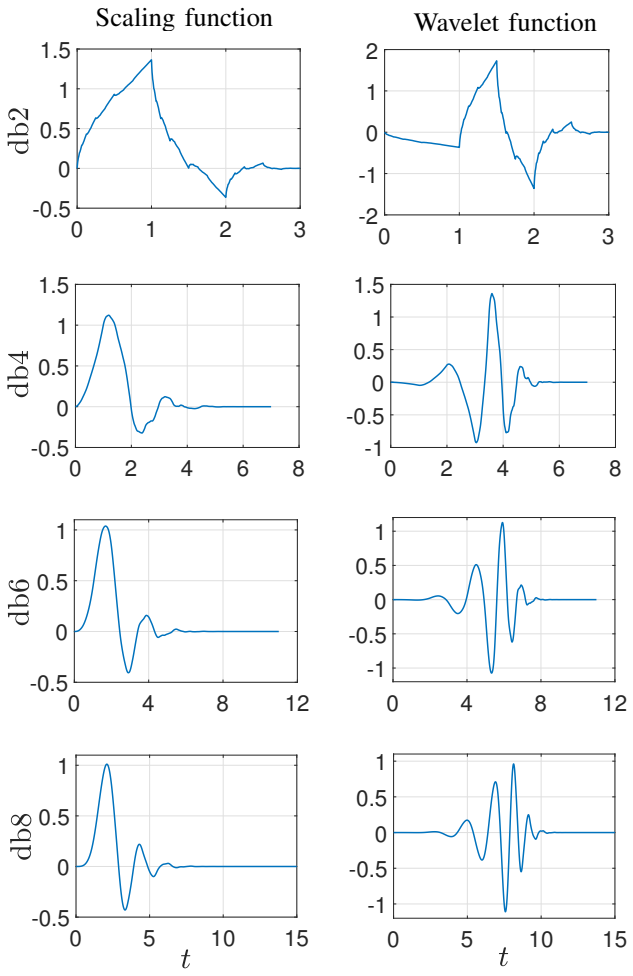

Fig. 2: Daubechies scaling and wavelet functions.

The solution procedure for the second-order problems given in this paper also dictates the use of the integral

$$p_{2,i}(1) = \int_0^1 p_{1,i}(t)dt. \tag{9}$$

The basic idea of HWCM is to transform the given differential equation into a system of algebraic equations with a finite number of variables. This transformation is achieved by making use of the collocation method where the collocation points are given by $t_l = (l - 0.5)\Delta t\,, l = 1, 2, ...2M\,, \Delta t = 1/(2M)$.

To solve Eq. (6) with the given boundary conditions, we first approximate the highest derivative appearing in the equation, $u''(t)$, in terms of Haar wavelets as

$$u''(t) = \sum_{i=1}^{2M} a_i h_i(t) \tag{10}$$

and integrate it twice to obtain lower derivatives $u'(t)$ and $u(t)$. The obtained approximations are discretized at the collocation points and substituted back to Eq. (6). This yields a system of nonlinear algebraic equations

$$F_l(a_1, a_2, \ldots, a_{2M}) = 0\,, \quad l = 1, 2, \ldots, 2M\,, \tag{11}$$

where a_i are the wavelet coefficients to be determined. The required unknown function is then computed by substituting a_i in its Haar approximation. The solution procedure also makes use of the Jacobian matrix, which is given by $S = \frac{\partial F_l}{\partial a_i}$.

The Newton-Raphson method is used to solve the system of equations (11). For the ν^{th} iteration, this system is of the form

$$\mathbf{S}^{(\nu)}\Delta a^{(\nu)} = -\mathbf{F}^{(\nu)} \tag{12}$$

where $\Delta a^{(\nu)}$ and $\mathbf{F}^{(\nu)}$ are vectors with elements $\Delta a^{(\nu)} = a_i^{(\nu+1)} - a_i^{(\nu)}$, $\mathbf{F}^{(\nu)} = F_l^{(\nu)}$, and $\mathbf{S}^{(\nu)} = S_l^{(\nu)}$ respectively. The solution of this equation is given by

$$\Delta a^{(\nu)} = -\mathbf{F}^{(\nu)}/\mathbf{S}^{(\nu)}. \tag{13}$$

This method is initiated at $J = 0$ and the level of resolution of Haar wavelet increases with each iteration. Thus the size of $\mathbf{S}, \mathbf{F}$ and Δa doubles with each iteration.

In this comparative study, since the exact solution of all problems under consideration is known, the accuracy of the Haar solution is estimated as

$$L_\infty = max|u_j^e - u_j^h| \tag{14}$$

where u_j^e and u_j^h are the exact solution and Haar solution at collocation points t_j , $1 \le j \le 2M$ The rate of convergence of the solution is determined using the following relation

$$\sigma(\nu) = \frac{L_\infty^{\nu-1}}{L_\infty^{\nu}} \quad \nu = 2, 3, ... \tag{15}$$

where $L_\infty^{\nu-1}$ and L_∞^{ν} are the absolute errors at resolution level $\nu - 1$ and ν respectively.

B. Wavelet-Galerkin method (WGM):

The wavelet-Galerkin method is a combination of orthonormal wavelet bases with the Galerkin method. At this juncture, an alternative to classical polynomial or trigonometric bases, the Daubechies wavelets (which are orthonormal bases for $L^2(\mathbb{R})$) are used to construct Galerkin bases. In WGM, it is important to compute the connection coefficients at a particular level of resolution of a Daubechies wavelet of a certain order. They are basically integrals where the integrands are products of Daubechies wavelet bases and their derivatives or integrals. In general, connection coefficients at a particular resolution of a certain order of Daubechies wavelet are necessary to achieve an acceptable approximate solution of a differential equation. The Galerkin method in conjunction with wavelet basis results in sparse matrices with bounded condition number (or low condition number). To illustrate the method, we consider the formulation of the Galerkin method for a general one-dimensional differential equation.

$$Lu(t) = f(t)\,, \quad 0 \le t \le 1\,, \tag{16}$$

with boundary conditions

$$u(0) = a\,, \quad u(1) = b\,. \tag{17}$$

The approximate solution of (16) is

$$u_S = \sum_{k\in\Lambda} x_k v_k \in S\,. \tag{18}$$

The reduced system of equations is given by

$$\sum_{k\in\Lambda} \langle Lv_k, v_j\rangle x_k = \langle f, v_j\rangle\,, \quad \forall j \in \Lambda \tag{19}$$

which is in matrix form

$$AX = Y\,. \tag{20}$$

The idea of selecting a wavelet basis for the Galerkin method emerges due to the two major requirements on the matrix A in (20): (i) we expect A to have a small condition number in order for the solution to be stable, and (ii) the matrix A should be sparse in order to obtain computational efficiency. Thus, the approximation solution (18) is rewritten in terms of wavelet basis $\psi_{j,k}$ as follows

$$u_S = \sum_{(j,k)\in\Lambda} x_{j,k}\psi_{j,k}\,,\ \text{where}\ \ \psi_{j,k}(t) = 2^{j/2}\psi(2^j t - k)\,. \tag{21}$$

The system (19) takes the form

$$\sum_{(j,k)\in\Lambda} \langle L\psi_{j,k}, \psi_{l,m}\rangle x_{j,k} = \langle f, \psi_{l,m}\rangle\,, \quad \forall\,(l,m)\in\Lambda\,. \tag{22}$$

The matrix form of (22) is

$$AX = Y \tag{23}$$

where the vectors $X = (x_{j,k})_{(j,k)\in\Lambda}$, $Y = (y_{l,m})_{(l,m)\in\Lambda}$, $y_{l,m} = \langle f, \psi_{l,m}\rangle$ and the matrix $A = [a_{l,m;j,k}]_{(l,m),(j,k)\in\Lambda}$, $a_{l,m;j,k} = \langle L\psi_{j,k}, \psi_{l,m}\rangle$ with row indexed by $(l,m)\in\Lambda$ and column indexed by $(j,k)\in\Lambda$. The details of construction of connection coefficients are given as an appendix to the paper. We computed the connection coefficients for various genus L of Daubechies wavelets at different scales using [21].

IV. Applications

In fulfilment of the objective stated in Section I, we have considered two-point nonlinear boundary value problems and discussed the method to tackle various forms of nonlinearities using HWCM and WGM through three case studies.

Example 1.

$$u''(t) = 2u^3(t)\,, \tag{24}$$

$$u(0) = 1\,, \qquad u(1) = \frac{1}{2}\,. \tag{25}$$

Method 1 (WGM): The nonlinear term $u^3(t)$ in Eq.(24) is linearized using the quasilinearization technique resulting in

$$u''_{r+1}(t) - 6u_r^2(t)u_{r+1}(t) = -4u_r^3(t) \tag{26}$$

with boundary conditions

$$u_{r+1}(0) = 1\,, \qquad u_{r+1}(1) = \frac{1}{2}\,. \tag{27}$$

Let the wavelet expansion for the unknown function $u(t)$ of Eq.(26) be

$$u_{r+1}(t) = \sum_{k=1-L}^{2^j} c_k 2^{j/2}\phi(2^j t - k) \tag{28}$$

where c_k are the unknown Daubechies wavelet filter coefficients. Substituting Eq.(28) in Eq.(26) we obtain

$$\begin{aligned}\tfrac{d^2}{dt^2}\textstyle\sum_k c_k 2^{j/2}\phi(2^j t-k) - 6u_r^2(t)\textstyle\sum_k c_k 2^{j/2}\phi(2^j t-k)\\ = -4u_r^3(t)\end{aligned} \tag{29}$$

We use the substitution $y = 2^j t$, $C_k = 2^{j/2}c_k$ so that $\frac{d^n}{dt^n} = 2^{nj}\frac{d^n}{dy^n}$, $n\in\mathbb{Z}_+$. Equation (29) simplifies to

$$\sum_k C_k 2^{2j}\phi''(y-k) - 6u_r^2(t)\sum_k C_k\phi(y-k) = -4u_r^3(t)\,. \tag{30}$$

Multiplying $\phi(y-p)$ on both sides of Eq.(30) and integrating,

$$\begin{aligned}\textstyle\sum_k C_k 2^{2j}\int\phi''(y-k)\phi(y-p)dy\\ -6u_r^2(t)\textstyle\sum_k C_k\int\phi(y-k)\phi(y-p)dy\\ = -4u_r^3(t)\int\phi(y-p)dy\end{aligned} \tag{31}$$

$$\implies\quad 2^{2j}\sum_k C_k\Omega^{0,2}_{k-p} - 6u_r^2(t)\sum_k C_k\delta_{kp} = -4u_r^3(t) \tag{32}$$

$$\text{or}\qquad 2^{2j}\sum_k C_k\Omega^{0,2}_{k-p} - 6u_r^2(t)C_p = -4u_r^3(t) \tag{33}$$

where

$$\Omega^{0,2}_{k-p} = \int\phi''(y-k)\phi(y-p)dy \tag{34}$$

$$\delta_{kp} = \int\phi(y-k)\phi(y-p)dy \tag{35}$$

The boundary conditions Eq.(27) implies

$$u_{r+1}(0) = \sum_k C_k\phi_k(0) = 1\,, \tag{36}$$

$$u_{r+1}(1) = \sum_k C_k\phi_k(1) = \frac{1}{2}\,. \tag{37}$$

Equations (36)-(37) represents the relation of the unknown coefficients c_k. On taking the inner product of $\phi_p(0)$ and $\phi_p(1)$ respectively, the Eq.(36) and Eq.(37) reduces to

$$\sum_k C_k\delta_{kp}(0) = 1\,, \tag{38}$$

$$\sum_k C_k\delta_{kp}(1) = \frac{1}{2}\,. \tag{39}$$

The first and last equations of Eq.(33) are replaced by Eq.(38) and Eq.(39). The modified system is solved by using Daubechies scaling function with $L = 6\ \ \&\ 12$ at different resolution levels j. The Daubechies scaling function at $L = 6$ and various dyadic points t is displayed in Table I.

Method 2 (HWCM): In solving Eq.(24) with HWCM, the highest derivative term $u''(t)$ is approximated in terms of Haar wavelets as

$$u''(t) = \sum_{i=1}^{2M} a_i h_i(t) \tag{40}$$

where a_i are Haar coefficients to be determined. The lower order derivatives $u'(t)$ and $u(t)$ are subsequently derived using integration.
On integrating Eq.(40) and using the given boundary conditions, we obtain

$$u'(t) = \sum_{i=1}^{2M} a_i\left(p_{1,i}(t) - p_{2,i}(1)\right) - \frac{1}{2} \tag{41}$$

$$u(t) = \sum_{i=1}^{2M} a_i\left(p_{2,i}(t) - tp_{2,i}(1)\right) + 1 - \frac{t}{2} \tag{42}$$

Eq.(24) takes the form

$$F_l = u''(t_l) - 2(u(t_l))^3 \tag{43}$$

and the elements of the matrix S are given by

$$S(i,l) = \frac{\partial u''(t_l)}{\partial a_i} - 6(u(t_l))^2 \frac{\partial u(t_l)}{\partial a_i} \tag{44}$$

substituting the values of $u_l(t)$ and $u_l''(t)$ according to Eq.(40) and Eq.(42),

$$\mathbf{F} = \sum_{i=1}^{2M} a_i h_i(t) - 2\left(\sum_{i=1}^{2M} a_i(p_{2,i}(t) - tp_{2,i}(1)) + 1 - \frac{t}{2}\right)^3 \tag{45}$$

$$\mathbf{S} = h_i(t) - 6\left(\sum_{i=1}^{2M} a_i(p_{2,i}(t) - tp_{2,i}(1)) + 1 - \frac{t}{2}\right)^2 (p_{2,i}(t) - tp_{2,i}(1)) \tag{46}$$

Equations (45) and (46) are substituted in Eq (13) and solved according to the procedure outlined previously. Table II gives the comparison of wavelet-Galerkin solution obtained by $db6$ with four iterations and Haar wavelet collocation method with the exact solution (Exact solution is $u(t) = 1/(1+t)$). The proposed method assures the accuracy of the results even for a lower resolution level as shown in Table II. The accuracy of the solution can be improved as the genus of the wavelet is increased. From the table, it is clear that the accuracy of the HWCM outperforms that of the WGM for a similar J value.

The comparison of the WGM for $db3$ and $db6$ and HWCM with the exact solution of Eq.(24) are plotted in Fig. 4. For an accurate picture of the scale of error in the two methods, the absolute errors obtained in the solution by both methods are plotted in the same figure with different axes. The absolute error in WGM is plotted on the left-hand axis using a dashed line, and the absolute error in HWCM is plotted on the the right-axis with a solid line. It is clearly observed that the error in HWCM is of the order 10^{-2} less than that in WGM. The absolute error and the rate of convergence for different values of J for the Haar solution of Eq.(24) are shown in Table III. The theoretical rate of convergence for HWCM is $\sigma = 4$, and from the table it is clear that the rate of convergence for the solution of Eq.(24) approaches the theoretical value for higher J values. Fig.3 plots the values of Haar coefficients a_i for $J = 4, 5$. The figure demonstrates one of the desirable properties of Haar wavelets which is the fact that the coefficients for higher i values tend to be close to zero. This property ensures that the Haar solution is accurate with minimal number of coefficients.

Example 2.

$$u''(t) + u'(t) + u^2(t) = t^4 + 2t + 2\,, \tag{47}$$

$$u(0) = 0\,, \quad u(1) = 1\,. \tag{48}$$

Method 1 (WGM): The quasilinearized form of Eq.(47) is

$$u''_{r+1}(t) + u'_{r+1}(t) + 2u_r(t)u_{r+1}(t) = u_r^2(t) + t^4 + 2t + 2 \tag{49}$$

$$u_{r+1}(0) = 0\,, \quad u_{r+1}(1) = 1\,. \tag{50}$$

TABLE I: Daubechies scaling function at $L = 6$.

t	$\phi(t)$	t	$\phi(t)$
0.000	0.0	2.625	-0.03693836
0.125	0.133949835	2.750	-0.040567571
0.250	0.284716624	2.875	0.037620632
0.375	0.422532739	3.000	0.095267546
0.500	0.605178468	3.125	0.062104053
0.625	0.743571274	3.250	0.02994406
0.750	0.89811305	3.375	0.011276602
0.875	1.090444005	3.500	-0.031541303
1.000	1.286335069	3.625	-0.013425276
1.125	1.105172581	3.750	0.003025131
1.250	0.889916048	3.875	-0.002388515
1.375	0.724108826	4.000	0.004234346
1.500	0.441122481	4.125	0.001684683
1.625	0.30687191	4.250	-0.001596798
1.750	0.139418882	4.375	0.000149435
1.875	-0.125676646	4.500	0.000210945
2.000	-0.385836961	4.625	-7.95485E-05
2.125	-0.302911152	4.750	1.05087E-05
2.250	-0.202979935	4.875	5.23519E-07
2.375	-0.158067602	5.000	-3.16007E-20
2.500	-0.014970591		

TABLE II: Comparison of wavelet-Galerkin solution using $db6$ and Haar wavelet solution of Eq.(24) fixing level of resolution of both wavelets to 8.

t	**WGM**	**HWCM**	**Exact solution**
0.0	1.0000000000	1.000000000	1.0000000000
0.1	0.9090966379	0.909090738	0.9090909091
0.2	0.8333423052	0.833333081	0.8333333333
0.3	0.7692413844	0.769230488	0.7692307692
0.4	0.7142968303	0.714285435	0.7142857143
0.5	0.6666773884	0.666666410	0.6666666667
0.6	0.6250095846	0.624999779	0.6250000000
0.7	0.5882431173	0.588235119	0.5882352941
0.8	0.5555611085	0.555555433	0.5555555556
0.9	0.5263186892	0.526315725	0.5263157895
1.0	0.5000000000	0.500000000	0.5000000000

Using the wavelet-Galerkin procedure as explained in Example 1, Eq.(49) reduces to

$$2^{2j}\sum_k C_k\Omega^{0,2}_{k-p} + 2^j\sum_k C_k\Omega^{0,1}_{k-p} + 2u_r(t)\sum_k C_k\delta_{kp} = u_r^2(t) + \sum_{i=0}^4 \tfrac{g_i}{2^{ji}} M_p^i \tag{51}$$

or

$$2^{2j}\sum_k C_k\Omega^{0,2}_{k-p} + 2^j\sum_k C_k\Omega^{0,1}_{k-p} + 2u_r(t)C_p = u_r^2(t) + \sum_{i=0}^4 \tfrac{g_i}{2^{ji}} M_p^i \tag{52}$$

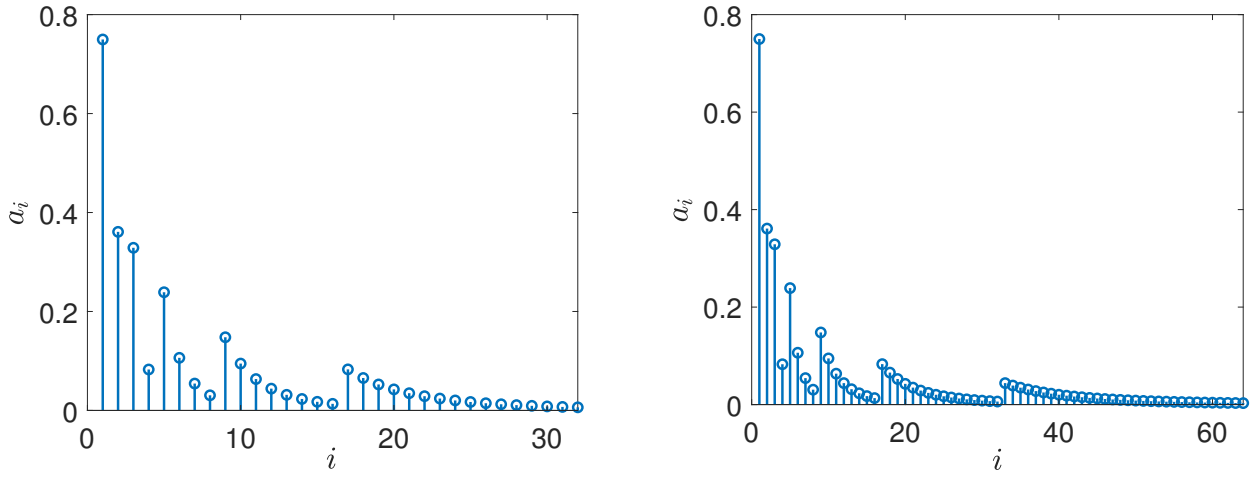

(a) $J = 4$ (b) $J = 5$

Fig. 3: Haar coefficients for the solution of Eq.(24) at different J values.

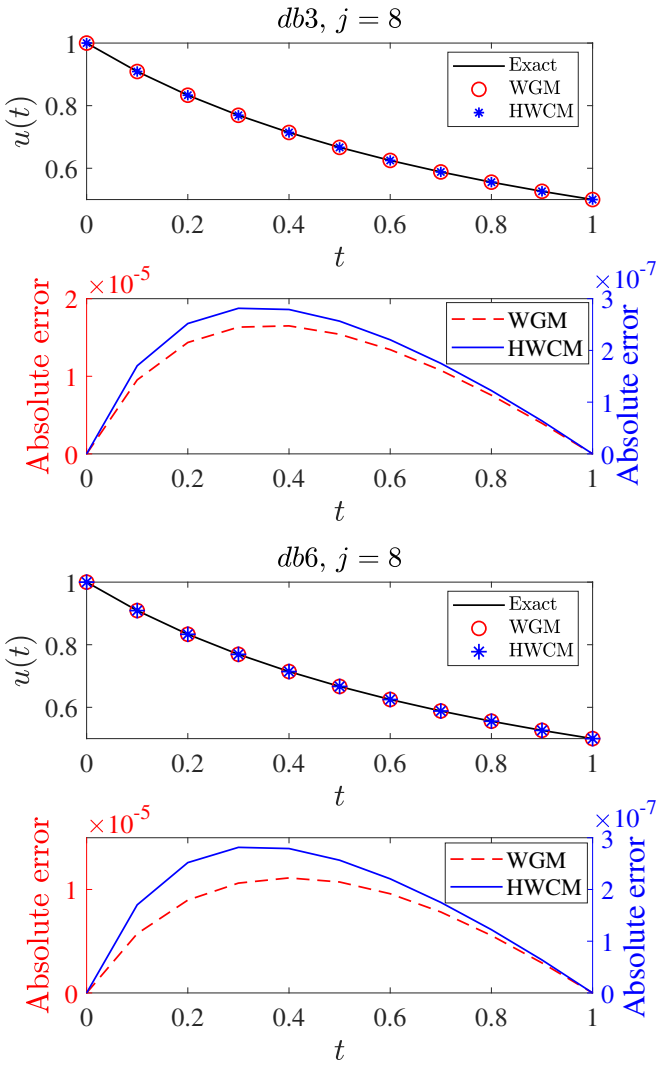

Fig. 4: Comparison of wavelet-Galerkin and Haar solution of Eq.(24) with the exact solution along with the absolute error using WGM (left-hand axis, dashed line) and HWCM (right-hand axis, solid line).

TABLE III: Error estimate Δ and rate of convergence σ for Haar solution of Eq (24).

J	Δ	σ
3	7.1682607157E-05	3.8226525089
4	1.8076627278E-05	3.9654857099
5	4.5324611592E-06	3.9882586178
6	1.1338311336E-06	3.9974746016
7	2.8349851166E-07	3.9994253479
8	7.0877611113E-08	3.9998316423
9	1.7719554379E-08	3.9999657777

where

$$\Omega_{k-p}^{0,2} = \int \phi''(y-k)\phi(y-p)dy \tag{53}$$

$$\Omega_{k-p}^{0,1} = \int \phi'(y-k)\phi(y-p)dy \tag{54}$$

$$\delta_{kp} = \int \phi(y-k)\phi(y-p)dy \tag{55}$$

$$M_p^i = \int y^i \phi(y-p)dy \tag{56}$$

and $g = [2, 2, 0, 0, 1]$. The relevant boundary conditions Eq.(50) simplifies to

$$\sum_k C_k \delta_{kp}(0) = 0 \tag{57}$$

$$\sum_k C_k \delta_{kp}(1) = 1 \tag{58}$$

The system Eq.(52) is modified by replacing the first and last equations by Eq.(57) and Eq.(58) respectively, and solved for C_k by using Daubechies scaling function with $L = 12$ & 16 for resolution level $j = 10$.

Method 2 (HWCM): Using the approach discussed previously, the required functions $u(t)$, $u'(t)$ and $u''(t)$ are approximated using Haar wavelets as

$$u''(t) = \sum_{i=1}^{2M} a_i h_i(t) \tag{59}$$

$$u'(t) = \sum_{i=1}^{2M} a_i \left(p_{1,i}(t) - p_{2,i}(1)\right) + 1 \tag{60}$$

$$u(t) = \sum_{i=1}^{2M} a_i \left(p_{2,i}(t) - tp_{2,i}(1)\right) + t \tag{61}$$

Discretization of Eq.(47) at collocation points results in

$$F_l = u''(t_l) + u'(t_l) + (u(t_l))^2 - t_l^4 - 2t - 2 \tag{62}$$

and the Jacobian S takes the form

$$S(i,l) = \frac{\partial u''(t_l)}{\partial a_i} + \frac{\partial u'(t_l)}{\partial a_i} + 2u(t_l)\frac{\partial u(t_l)}{\partial a_i} \tag{63}$$

The Haar approximations are substituted into F_l and $S(i,l)$ to obtain

$$\begin{aligned}\mathbf{F} =& \sum_{i=1}^{2M} a_i h_i(t) - \sum_{i=1}^{2M} a_i (p_{1,i}(t) - tp_{2,i}(1)) \\ &+ \left(\sum_{i=1}^{2M} (p_{2,i}(t) - tp_{2,i}(1) + t\right)^2 - t^4 - 2t - 1\end{aligned} \tag{64}$$

$$\begin{aligned}\mathbf{S} =& h_i(t) + p_{1,i}(t) - tp_{2,i}(1) + 2(p_{2,i}(t) - tp_{2,i}(1)) \\ &\left(\sum_{i=1}^{2M} (p_{2,i}(t) - tp_{2,i}(1) + t\right)\end{aligned} \tag{65}$$

and the solution for the desired level of resolution J is obtained as previously discussed.

The wavelet-Galerkin solution of Eq.(47) using $db8$ (four iterations) along with the Haar wavelet solution and the analytical solution ($u(t) = t^2$) are presented in Table IV. As can be seen from the provided table, the Haar wavelet solution precisely matches the analytical solution for this problem, and hence only the error in WGM solution is presented. The comparison plots of the exact solution and HWCM solution with WGM solutions for two different orders of Daubechies wavelets $db6$ and $db8$ are shown in Fig. 5. It is noticed that the accuracy of the WGM solution increases with increasing the order of wavelet from $db6$ to $db8$.

Example 3.

$$u''(t) + u(t)\left(u'(t) - 1\right) = \left(u'(t)\right)^2, \tag{66}$$

$$u(0) = 1, \qquad u(1) = e. \tag{67}$$

Method 1 (WGM): Quasilinearization technique to Eq.(66) implies

$$\begin{aligned}&u''_{r+1}(t) + \left(u_r(t) - 2u'_r(t)\right) u'_{r+1}(t) \\ &+ \left(u'_r(t) - 1\right) u_{r+1}(t) = u_r(t)u'_r(t) - \left(u'_r(t)\right)^2\end{aligned} \tag{68}$$

with the boundary conditions

$$u_{r+1}(0) = 1, \qquad u_{r+1}(1) = e. \tag{69}$$

TABLE IV: Comparison of wavelet-Galerkin solution using $db8$ and Haar solution of Eq.(47) at level of resolution = 10.

t	WGM	HWCM	Exact solution	Absolute error (WGM)
0.0	0.0	0.0	0.0	0
0.1	0.0100003618	0.010000000	0.010000000	3.618E-07
0.2	0.0400006461	0.040000000	0.040000000	6.461E-07
0.3	0.0900008362	0.090000000	0.090000000	8.362E-07
0.4	0.1600009258	0.160000000	0.160000000	9.258E-07
0.5	0.2500009178	0.250000000	0.250000000	9.178E-07
0.6	0.3600008234	0.360000000	0.360000000	8.234E-07
0.7	0.4900006608	0.490000000	0.490000000	6.608E-07
0.8	0.6400004526	0.640000000	0.640000000	4.526E-07
0.9	0.8100002239	0.810000000	0.810000000	2.239E-07
1.0	1.0000000000	1.000000000	1.000000000	0

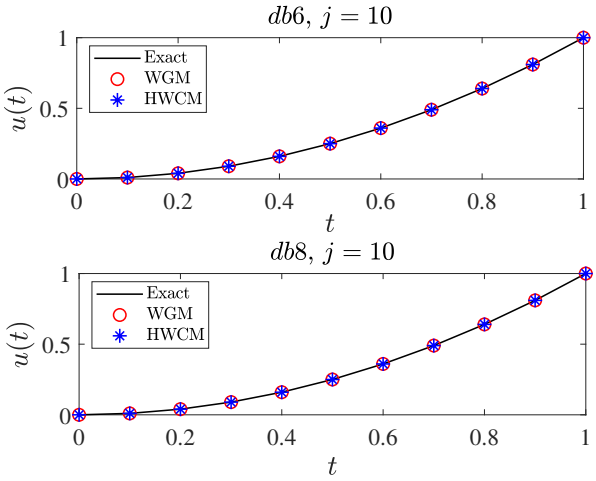

Fig. 5: Comparison of wavelet-Galerkin and Haar solution of Eq.(47) with the exact solution.

On implementation of wavelet-Galerkin method to Eq.(68) results in the following system

$$\begin{aligned}&2^{2j}\textstyle\sum_k C_k \Omega^{0,2}_{k-p} + \left(u_r(t) - 2u'_r(t)\right) 2^j \textstyle\sum_k C_k \Omega^{0,1}_{k-p} \\ &+ \left(u'_r(t) - 1\right) \textstyle\sum_k C_k \delta_{kp} = u_r(t)u'_r(t) - \left(u'_r(t)\right)^2\end{aligned} \tag{70}$$

or

$$\begin{aligned}&2^{2j}\textstyle\sum_k C_k \Omega^{0,2}_{k-p} + \left(u_r(t) - 2u'_r(t)\right) 2^j \textstyle\sum_k C_k \Omega^{0,1}_{k-p} \\ &+ \left(u'_r(t) - 1\right) C_p = u_r(t)u'_r(t) - \left(u'_r(t)\right)^2\end{aligned} \tag{71}$$

where

$$\Omega^{0,2}_{k-p} = \int \phi''(y-k)\phi(y-p)dy \tag{72}$$

$$\Omega^{0,1}_{k-p} = \int \phi'(y-k)\phi(y-p)dy \tag{73}$$

$$\delta_{kp} = \int \phi(y-k)\phi(y-p)dy \tag{74}$$

Likewise, the boundary conditions Eq.(69) takes the form

$$\sum_k C_k \delta_{kp}(0) = 1 \tag{75}$$

$$\sum_k C_k \delta_{kp}(1) = e \tag{76}$$

Daubechies wavelets of order $db3$ and $db6$ with $j = 8$ are used for the computation of solution for the given problem.

Method 2 (HWCM): For the solution of Eq.(66) using Haar wavelets, the required unknown functions are approximated as follows

$$u''(t) = \sum_{i=1}^{2M} a_i h_i(t) \tag{77}$$

$$u'(t) = \sum_{i=1}^{2M} a_i \left(p_{1,i}(t) - p_{2,i}(1)\right) + e - 1 \tag{78}$$

$$u(t) = \sum_{i=1}^{2M} a_i \left(p_{2,i}(t) - t p_{2,i}(1)\right) + te - t + 1 \tag{79}$$

The discretized form of Eq.(66) is

$$F_l = u''(t_l) + u(t_l)(u'(t_l) - 1) - (u'(t_l))^2 \tag{80}$$

and the Jacobian is written as

$$\begin{aligned} S(i,l) =& \frac{\partial u''(t_l)}{\partial a_i} + u(t_l)\frac{\partial u'(t_l)}{\partial a_i} \\ &+ (u'(t_l) - 1)\frac{\partial u(t_l)}{\partial a_i} - 2u'(t_l)\frac{\partial u'(t_l)}{\partial a_i} \end{aligned} \tag{81}$$

Haar approximations are substituted into the above equations to get

$$\begin{aligned} \mathbf{F} =& \sum_{i=1}^{2M} a_i h_i(t) - \left(\sum_{i=1}^{2M} a_i (p_{1,i}(t) - p_{2,i}(1) + e - 1\right)^2 \\ &+ \left(\sum_{i=1}^{2M} a_i (p_{1,i}(t) - p_{2,i}(1) + e - 2\right) \\ &\left(\sum_{i=1}^{2M} a_i (p_{2,i}(t) - t p_{2,i}(1) + 1 + te - t\right) \end{aligned} \tag{82}$$

$$\begin{aligned} S =& h_i(t) + \left(\sum_{i=1}^{2M} a_i (p_{1,i}(t) - p_{2,i}(1)) - e + 2\right) \\ &(p_{2,i}(t) - t p_{2,i}(1)) + (p_{1i}(t) - p_{2,i}(1)) \\ &\left(\sum_{i=1}^{2M} a_i (p_{2,i}(t) - t p_{2,i}(1) + 1 + te - t\right) \\ &- 2(p_{1i}(t) - p_{2,i}(1)) \left(\sum_{i=1}^{2M} a_i (p_{1,i}(t) - p_{2,i}(1) + e - 1\right) \end{aligned} \tag{83}$$

The Haar coefficients a_i are derived using (13), (82) and (83), and the solution for the required J value is obtained iteratively as described in Section III. The numerical solutions and the closed form solution ($u(t) = e^t$) are presented in Table V. The obtained solution for both methods is in good agreement with the analytical solution but it should be noted that HWCM is once again superior to WGM in terms of accuracy of the solution. Fig. 6 plots the exact solution with solutions obtained by HWCM and WGM. The absolute errors in the solution procedure for both methods are plotted using two different axes in the same figure. The left-hand axis plots the error in WGM using a dashed line, whereas the right-hand axis plots the error in HWCM with a solid line. From the figure it is evident that the HWCM has a better accuracy with an absolute error 10^{-2} orders less than the WGM solution. Table VI shows the absolute errors and rate of convergence of Haar wavelet solution for different levels of resolution J. It can be clearly seen that the error in the Haar solution decreases greatly with increasing J, and the rate of convergence σ approaches the theoretical value of $\sigma = 4$ for higher values of J. The Haar coefficients a_i for different J values are shown in Fig.7. It is once again observed that as i increases, the value of a_i tends close to 0. This sparsity of the involved matrices is one of the reasons for the efficiency of Haar wavelets in the solution of differential equations.

TABLE V: Comparison of wavelet-Galerkin solution using $db6$ and Haar solution of Eq.(66) at level of resolution = 8.

t	WGM	HWCM	Exact solution
0.0	1.0000000000	1.0000000000	1.0000000000
0.1	1.1051676974	1.1051708263	1.1051709181
0.2	1.2213963204	1.2214025795	1.2214027582
0.3	1.3498493237	1.3498585496	1.3498588076
0.4	1.4918125459	1.4918243715	1.4918246976
0.5	1.6487070838	1.6487208927	1.6487212707
0.6	1.8221035268	1.8221183941	1.8221188004
0.7	2.0137376947	2.0137523068	2.0137527075
0.8	2.2255280418	2.2255405822	2.2255409285
0.9	2.4595949090	2.4596028886	2.4596031112
1.0	2.7182818285	2.7182818285	2.7182818285

TABLE VI: Error estimate Δ and rate of convergence σ for the Haar solution of Eq.(66).

J	Δ	σ
3	1.0475018846E-04	3.9687451386
4	2.6210363965E-05	3.9965178888
5	6.5509939886E-06	4.0009751209
6	1.6378200764E-06	3.9998251839
7	4.0944715928E-07	4.0000767847
8	1.0236227310E-07	3.9999811149
9	2.5590562557E-08	4.0000008937

V. Conclusion

In the present paper, three typical second-order differential equations with various nonlinearities have been tackled using the Daubechies wavelet-based Galerkin method and the Haar wavelet collocation method. The ease of implementation and the solution accuracy of both methods are examined. The important results have been summarized below:

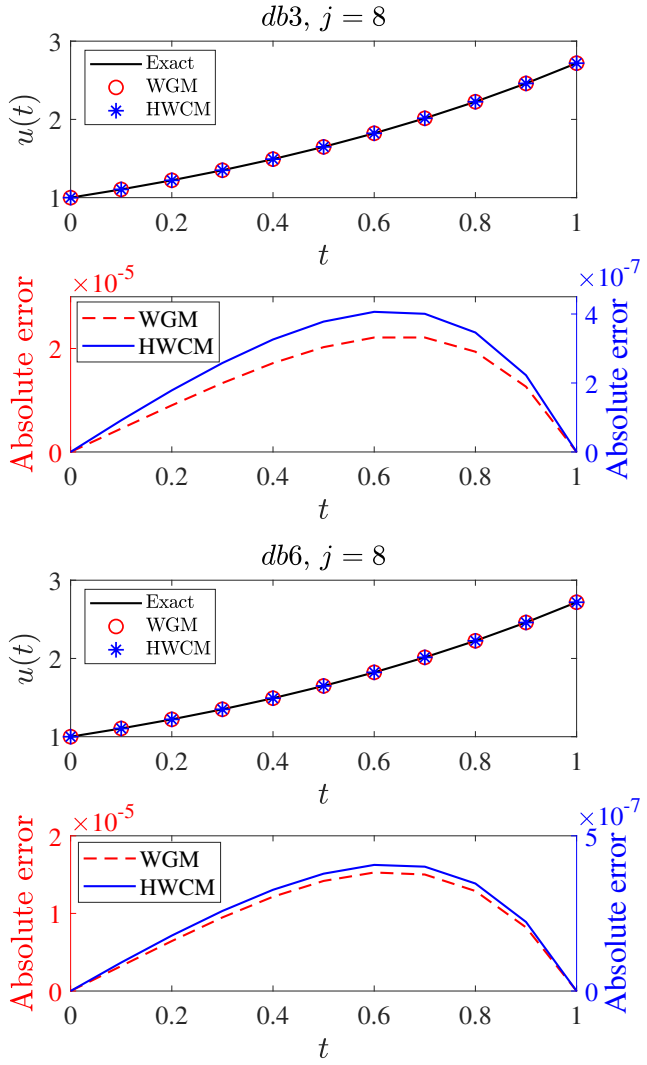

Fig. 6: Comparison of wavelet-Galerkin and Haar solution of Eq.(66) with the exact solution along with the absolute error using WGM (left-hand axis, dashed line) and HWCM (right-hand axis, solid line).

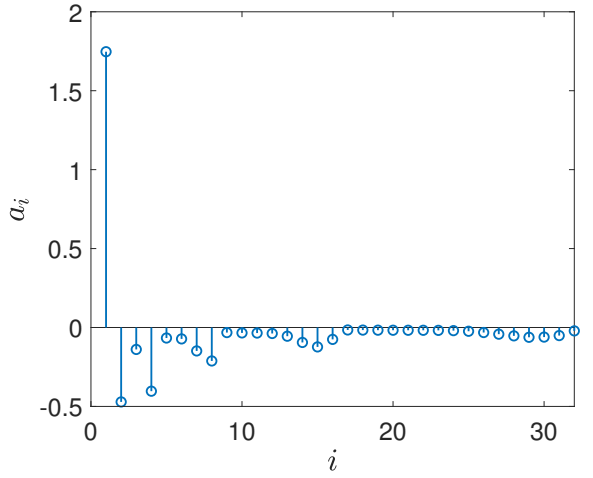

(a) $J = 4$

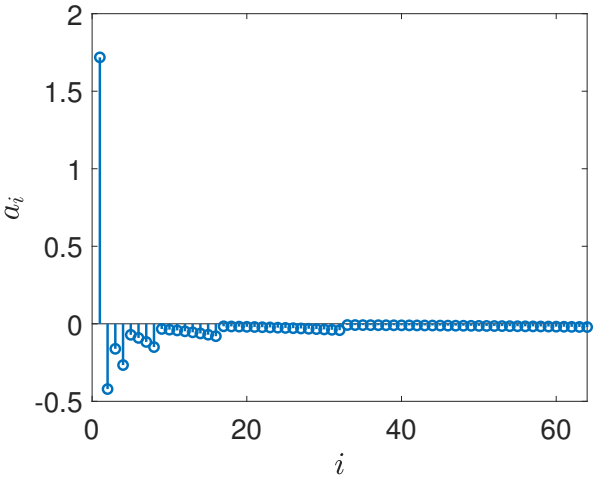

(b) $J = 5$

Fig. 7: Haar coefficients for the solution of Eq.(66) at $J = 4, 5$.

1) The Daubechies wavelets are orthogonal and sufficiently smooth but they cannot be expressed in terms of an explicit function, complicating the differentiation and integration procedures.
2) WGM proves to be efficient for solving boundary value problems when higher order wavelets are considered as basis functions. However, when confronted by higher-order differential equations with nonlinearity or singularity (Neumann or mixed boundary conditions), calculating the corresponding connection coefficients becomes very tedious.
3) Due to repeated computations of integrals of products of Daubechies wavelets and their derivatives, the solution procedure of WGM will take more computational time in these cases. On the other hand, the HWCM provides simple and convergent solution procedures with fast computations.
4) It is important to observe that, in WGM, the wavelet transform and its inverse are implemented on the discretized system of algebraic equations, while in HWCM the differential equation is approximated through wavelet series.
5) Due to the sparsity of transform matrices, HWCM has simple implementation and small computation costs which makes it more efficient than WGM. From a computational viewpoint, this study shows that the HWCM method is more efficient and easier to use than WGM.

APPENDIX

Two-term connection coefficients:

In solving a differential equation of the form

$$f\left(t, \frac{du}{dt}, \frac{d^2u}{dt^2}\right) = 0 \tag{84}$$

defined on a bounded interval $t \in [a, b]$ by wavelet-Galerkin method, it is required to determine the connection coefficients [9]. The two-term connection coefficients are defined as

$$\Omega_l^{d_1,d_2} = \int_{-\infty}^{\infty} \phi^{d_1}(t)\phi_l^{d_2}(t)dt \tag{85}$$

By taking d times derivatives of the Daubechies scaling function $\phi(t) = \sum_{k=0}^{L-1} p_k \phi(2t-k)$ where $p_k = \sqrt{2}c_k$, we

get

$$\phi^d(t) = 2^d \sum_{k=0}^{L-1} p_k \phi_k^d(2t) \tag{86}$$

where

$$\phi^d(t) := \frac{d^d \phi(t)}{dt^d} \tag{87}$$

Using Eq.(86) in Eq.(85) and changing variables, we obtain

$$\Omega_l^{d_1,d_2} = 2^{d_1+d_2-1} \sum_{m,n} p_m p_{n-2l+m} \int_{-\infty}^{\infty} \phi^{d_1}(t) \phi_n^{d_2}(t) dt \tag{88}$$

For various values of l and t, Eq.(88) gives a system of equations which is denoted in matrix form as

$$T\Omega^{d_1,d_2} = \frac{1}{2^{d-1}} \Omega^{d_1,d_2} \tag{89}$$

where Ω^{d_1,d_2} is unknown column vector with $2L-3$ components, $d = d_1 + d_2$ and

$$T = \sum_m p_m p_{n-2l+m} \,. \tag{90}$$

The system Eq.(89) is homogeneous and does not have a unique non-zero solution. To make the system inhomogeneous, a normalization equation is added (which is derived from the moment equation of the scaling function $\phi(t)$)

$$d! = (-1)^d \sum_l M_l^d \Omega_l^{0,d} \tag{91}$$

where M_i^k is kth moment of $\phi_i(t)$, defined as

$$M_i^k = \int_{-\infty}^{\infty} x^k \phi_i(t) dt \tag{92}$$

Thus, the system Eq.(89) will reduce to the form

$$\begin{pmatrix} T - \frac{1}{2^{d-1}} I \\ M^d \end{pmatrix} \Omega^{d_1,d_2} = \begin{pmatrix} 0 \\ d! \end{pmatrix} \tag{93}$$

where M^d is a row vector with all the M_l^d. The unique solution of this system will give the connection coefficients Ω^{d_1,d_2}.

REFERENCES

[1] C. Chen and C. Hsiao, "Haar wavelet method for solving lumped and distributed-parameter systems," *IEE Proceedings-Control Theory and Applications*, vol. 144, no. 1, pp. 87–94, 1997.

[2] Ü. Lepik, "Numerical solution of evolution equations by the Haar wavelet method," *Applied Mathematics and Computation*, vol. 185, no. 1, pp. 695–704, 2007.

[3] P. Chang and P. Piau, "Haar wavelet matrices designation in numerical solution of ordinary differential equations," *IAENG International Journal of Applied Mathematics*, vol. 38, no. 3, pp. 164–168, 2008.

[4] G. Hariharan and K. Kannan, "An overview of haar wavelet method for solving differential and integral equations," *World Applied Sciences Journal*, vol. 23, no. 12, pp. 1–14, 2013.

[5] Ö. Oruç, F. Bulut, and A. Esen, "Numerical solutions of regularized long wave equation by haar wavelet method," *Mediterranean Journal of Mathematics*, vol. 13, no. 5, pp. 3235–3253, 2016.

[6] S. Shiralashetti, A. Deshi, and P. M. Desai, "Haar wavelet collocation method for the numerical solution of singular initial value problems," *Ain Shams Engineering Journal*, vol. 7, no. 2, pp. 663–670, 2016.

[7] I. Daubechies, *Ten lectures on wavelets*. SIAM, 1992.

[8] R. Glowinski, W. M. Lawton, and E. Ravachol, M.and Tenenbaum, "Wavelets solution of linear and nonlinear elliptic, parabolic and hyperbolic problems in one space dimension," *In: R. Glowinsky, A. Lichnewsky, eds., Computing Methods in Applied Sciences and Engineering, SIAM*, pp. 55–120, 1990.

[9] A. Latto, H. L. Resnikoff, and E. Tenenbaum, "The evaluation of connection coefficients of compactly supported wavelets," in *Proceedings of the French-USA Workshop on Wavelets and Turbulence, Princeton University, June 1991*. Springer-Verlag, New York, 1992, pp. 76–89.

[10] C. H. Romine and B. W. Peyton, "Computing connection coefficients of compactly supported wavelets on bounded intervals (no. ornl/tm-13413)," *Oak Ridge National Lab., Mathematical Sciences Section, TN (United States)*, 1997.

[11] K. Amaratunga, J. R. Williams, S. Qian, and J. Weiss, "Wavelet-Galerkin solutions for one dimensional partial differential equations," *International Journal for Numerical Methods in Engineering*, vol. 37, no. 16, pp. 2703–2716, 1994.

[12] D. Lu, T. Ohyoshi, and L. Zhu, "Treatment of boundary conditions in the application of wavelet-Galerkin method to an SH wave problem," *International Journal of the Society of Materials Engineering for Resources*, vol. 5, no. 1, pp. 15–25, 1997.

[13] A. Choudhury and R. Deka, "Wavelet-Galerkin solutions of one dimensional elliptic problems," *Applied Mathematical Modelling*, vol. 34, no. 7, pp. 1939–1951, 2010.

[14] G. Priyadarshi and B. R. Kumar, "Wavelet galerkin method for fourth order linear and nonlinear differential equations," *Applied Mathematics and Computation*, vol. 327, pp. 8–21, 2018.

[15] P. Da Silva, J. Da Silva, and A. Garcia, "Daubechies wavelets as basis functions for the vectorial beam propagation method," *Journal of Electromagnetic Waves and Applications*, vol. 33, no. 8, pp. 1027–1041, 2019.

[16] D. Černá and V. Finěk, "Galerkin method with new quadratic spline wavelets for integral and integro-differential equations," *Journal of Computational and Applied Mathematics*, vol. 363, pp. 426–443, 2020.

[17] H. Bin Jebreen and I. Dassios, "A biorthogonal hermite cubic spline galerkin method for solving fractional riccati equation," *Mathematics*, vol. 10, no. 9, p. 1461, 2022.

[18] Y. Rostami, "An effective computational approach based on hermite wavelet galerkin for solving parabolic volterra partial integro differential equations and its convergence analysis," *Mathematical Modelling and Analysis*, vol. 28, no. 1, pp. 163–179, 2023.

[19] M. E. Köksal, "Recent developments of numerical methods for analyzing telegraph equations," *Archives of Computational Methods in Engineering*, pp. 1–19, 2023.

[20] T. Zhang, Y. Tian, M. Tade, and J. Utomo, "Comments on-the computation of wavelet-Galerkin approximation on a bounded interval," *International Journal for Numerical Methods in Engineering*, vol. 72, no. 2, pp. 244–251, 2007.

[21] J. Besora, "Galerkin wavelet method for global waves in 1D," Master's thesis, Royal Institute of Technology, Stockholm, Sweden, 2004.